Numerical Analysis of Planar Cam Follower Mechanisms

Gökhan KİPER[1], Chintien HUANG[2] and Eres SÖYLEMEZ[3]

Given planar cam profiles and follower types, this paper analyzes their displacement diagrams numerically. The algorithm is based on the concept that a cam and its follower must have a common normal at the contact point. Instead of using kinematic inversion, this paper directly calculates contact points in the fixed coordinate system. This paper demonstrates a straightforward approach for motion analysis when discrete cam profile data points and link lengths are available. We implement the method by using the spreadsheet program Microsoft Excel®, which is well-suited for dealing with discrete data points. The results given in this paper can easily be employed in reverse engineering applications and adapted in undergraduate curriculum.

Keywords: *Planar Cam Follower Mechanism, Cam Profile, Displacement Diagram, Spreadsheet Program*

1. Introduction

When designing cam-follower mechanisms, we usually begin with specifications of the displacement diagram, which relate the input and output motion, and then design cam profiles accordingly. However, in practice, we frequently encounter the reverse engineering problem of cam-follower mechanisms. Namely, given a cam-follower mechanism, it is desired to know the corresponding displacement diagram for the purpose of reproducing a cam piece or improving an existing design of the cam profile.

In practice, the customary way to determine the profile of a cam piece is to measure it via cam analysis devices. These devices simultaneously measure amount of cam rotation, velocity and acceleration and determine the cam profile via a translatory round or flat measuring probe [1-3]. The devices also measure velocity and acceleration. Some computer programs for these testing devices are available for further dynamic analysis [4]. In this paper, we seek to obtain the displacement diagram numerically only from measured discrete data points on the cam profile, without using the testing devices.

Wunderlich [5] solved the direct kinematics problem for the oscillating flat-faced follower case by assuming the contact points on the cam are expressed in terms of the cam rotation angle. Angeles and López-Cajún [6] investigated the kinematic analysis of cam mechanisms with oscillating/translating roller/flat-face followers, and they assumed the coordinates of discrete contact points on the cam are known in terms of the cam rotation angle. Reinholtz [7] investigated both cases where the cam profile is expressed either analytically or in terms of discrete point coordinates. The proposed solution in [7] was to first fit a cubic spline to the data and then to apply the described analytical method. Similarly, Fries and Rogers [8] fitted a series of fourth order polynomials to the numerical cam and follower profile coordinates and determined contact locations by applying an iterative search procedure. Fries and Rogers [8] used curve fitting rather than interpolation between data points because curve fitting provides some numerical smoothing of irregularities in the input data. Kirwan [9] constructed the displacement diagram of a cam follower mechanism when the cam profile is given graphically.

The synthesis of cam profiles has been extensively studied and is covered in most undergraduate mechanism textbooks. The analysis of cam-follower mechanisms, however, is lesser known and not introduced in undergraduate textbooks, even though it is a practical tool. This paper seeks to provide a systematic and straightforward approach for the numerical analysis of planar cam-follower mechanisms. Furthermore, we implement the algorithm by using the popular spreadsheet program Excel, which is well-suited for the purpose and can be used as an efficient tool for undergraduate education.

2. Previous Studies

The problem of determining the follower motion given discrete data points on the cam profile has been previously solved using kinematic inversion by Tutak and Söylemez [10], which was published in Turkish. In what follows, we summarize the formulation reported in Tutak and Söylemez's work [10]. The study sought to solve the problem of reproducing a cam piece. They started with finding the coordinates of the center of curvature $D(x_{D,n},y_{D,n})$ for each data point $C(x_n,y_n)$ on the cam profile by intersecting the perpendicular bisectors of line segments from (x_n,y_n) to the adjacent data points, (x_{n-1},y_{n-1}) and (x_{n+1},y_{n+1}). They also found the normal direction to the cam surface at (x_n,y_n) represented by the inclination angle of $\overrightarrow{DC}$, denoted by α_n. They then derived the necessary formulas and obtained the displacement diagrams for five different follower types:

[1] G. Kiper is with Dept. of Mechanical Engineering, İzmir Institute of Technology, 35430, İzmir, TURKEY, gokhankiper@iyte.edu.tr

[2] C. Huang is with Dept. of Mechanical Engineering, National Cheng Kung University, Tainan, TAIWAN, chuang@mail.ncku.edu.tw

[3] E. Söylemez is with Dept. of Mechanical Engineering, Middle East Technical University, 06800, Ankara, TURKEY, eres@metu.edu.tr

inline translating roller follower, offset translating roller follower, oscillating roller follower, translating flat-faced follower, and oscillating flat-faced follower.

Inline Translating Roller Follower

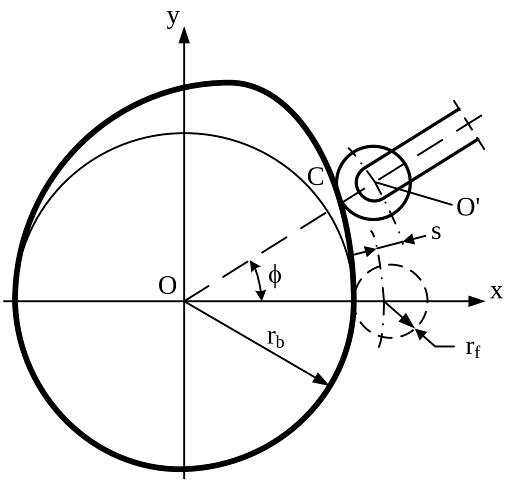

Fig. 1 Inline Translating Roller Follower Case [10]

As depicted in Fig. 1, let O, O', and C denote the cam rotation center, roller center, and point of contact, respectively. By kinematic inversion, the cam is fixed, and C(x,y) is assumed to be known as one of the discrete data points on the cam boundary. Let r_b denote the base circle radius of the cam, r_f the roller radius, r_c the distance $|\overrightarrow{OC}|$, ϕ_c the angle $\measuredangle\overrightarrow{OC}$, α the angle $\measuredangle\overrightarrow{CO'}$, r_p the distance $|\overrightarrow{OO'}|$, θ the cam rotation angle, and s the corresponding follower displacement. Assuming that r_b and r_f are known, we have

$$\overrightarrow{OC}+\overrightarrow{CO'}=\overrightarrow{OO'} \Rightarrow r_c e^{i\phi_c}+r_f e^{i\alpha}=r_p e^{i\theta} \tag{1}$$

Since all parameters in the left hand side of Eq. (1) are known, r_p and θ are found to be

$$\theta=\theta_p=\tan^{-1}\frac{y+r_f\sin\alpha}{x+r_f\cos\alpha} \tag{2}$$

$$r_p=\sqrt{r_c^{\,2}+r_f^{\,2}+2r_c r_f\cos(\phi_c-\alpha)} \tag{3}$$

Note that the curve given by $r_p e^{i\theta}$ is the pitch (prime) curve. The follower displacement s is:

$$s=r_p-r_f-r_b \tag{4}$$

Offset Translating Roller Follower

When r_b, r_f , and eccentricity e are known, we have

$$\theta=\theta_p+\sin^{-1}\frac{e}{r_p} \tag{5}$$

$$s=\sqrt{r_p^{\,2}-e^2}-\sqrt{(r_b+r_f)^2-e^2} \tag{6}$$

Oscillating Roller Follower

When r_b, r_f, r_r (the follower rocker arm length), and r_a (the distance between the revolute joints) are known, the cam rotation angle and follower angular displacement are, respectively,

$$\theta=\theta_p-\cos^{-1}\frac{r_a^{\,2}+r_p^{\,2}-r_r^{\,2}}{2r_a r_p} \tag{7}$$

$$\phi=\cos^{-1}\frac{r_a^{\,2}+r_r^{\,2}-r_p^{\,2}}{2r_a r_r}-\cos^{-1}\frac{r_a^{\,2}+r_r^{\,2}-(r_b+r_f)^2}{2r_a r_r} \tag{8}$$

Translating Flat-Faced Follower

In this case the cam rotation angle and follower displacement are, respectively,

$$\theta=\alpha=\tan^{-1}\frac{y-y_D}{x-x_D} \tag{9}$$

$$s=x\cos\theta+y\sin\theta-r_b \tag{10}$$

Oscillating Flat-Faced Follower

There are some typos for this case in [10]. After correction, the cam and follower angles for known r_b and r_a are

$$\theta=\phi_l+\sin^{-1}\frac{r_c\sin(\phi_c-\phi_l)}{r_a} \tag{11}$$

$$\phi=\cos^{-1}\frac{r_a^{\,2}+r_l^{\,2}-r_c^{\,2}}{2r_a r_l}-\sin^{-1}\frac{r_b}{r_a} \tag{12}$$

where

$$r_c=|\overrightarrow{OC}|=\sqrt{x^2+y^2}$$

$$\phi_c=\measuredangle\overrightarrow{OC}=\operatorname{atan2}(x,y)$$

$$\phi_l=\alpha-\pi/2$$

$$r_l=r_a\cos(\theta-\phi_l)-r_c\cos(\phi_c-\phi_l)$$

For the oscillating flat-faced follower case, there is an equivalent but more concise formulation using kinematic inversion without the need for defining r_l (distance of contact point C to the rotation center of follower). Referring to Fig. 2, we obtain the following by using the sine theorem for triangle OCQ and the outer angle rule:

$$\phi=\sin^{-1}\frac{r_c\cos(\phi_c-\alpha)}{r_a}-\sin^{-1}\frac{r_b}{r_a} \tag{13}$$

$$\theta=\phi+\phi_0+\alpha-\pi/2 \tag{14}$$

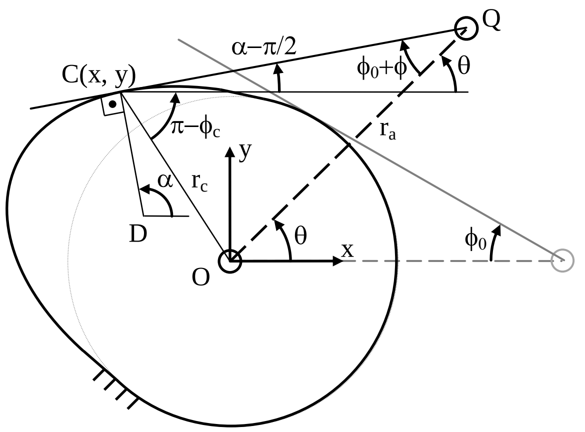

Fig. 2 Oscillating flat-faced follower case

3. Kinematic Analysis without Kinematic Inversion

Kinematic inversion may be tricky for practicing engineers and, especially, undergraduate students. Below we present a formulation without using kinematic inversion and compare it to the formulation summarized in Section 2.

We start by determining the normal direction to the cam profile at any data point. The data points may be given/measured in an arbitrarily oriented coordinate frame with its origin at the cam rotation center and in either Cartesian form (x_n,y_n) or polar form $r_n e^{i\phi_n}$, where $\phi_n = 2\pi n/N$, $0 \le n \le N-1$. Here N denotes the number of data points describing the cam profile. We use both Cartesian and polar coordinates of the data points in our calculations. The base circle radius r_b is determined as

$$r_b = \min_{0\le n\le N-1} r_n \tag{15}$$

It is possible to determine the location of the center of curvature D associated with the data point $C(x_n,y_n)$ using the expression for the coordinates of the center of the circumcenter of the triangle with vertices $(x_{n-1},y_{n-1}) \equiv r_{n-1}e^{i\phi_{n-1}}$, $(x_n,y_n) \equiv r_n e^{i\phi_n}$, and $(x_{n+1},y_{n+1}) \equiv r_{n+1}e^{i\phi_{n+1}}$ [11]:

$$x_{D,n} = \frac{r_{n-1}^2(y_{n+1}-y_n)+r_{n+1}^2(y_n-y_{n-1})+r_n^2(y_{n-1}-y_{n+1})}{2\left[x_{n-1}(y_{n+1}-y_n)+x_{n+1}(y_n-y_{n-1})+x_n(y_{n-1}-y_{n+1})\right]} \tag{16}$$

$$y_{D,n} = \frac{r_{n-1}^2(x_n-x_{n+1})+r_{n+1}^2(x_{n-1}-x_n)+r_n^2(x_{n+1}-x_{n-1})}{2\left[x_{n-1}(y_{n+1}-y_n)+x_{n+1}(y_n-y_{n-1})+x_n(y_{n-1}-y_{n+1})\right]} \tag{17}$$

Then, the normal direction at $C(x_n,y_n)$ is given by the inclination angle α_n with respect to the horizontal axis as

$$\alpha_n = \operatorname{atan2}\left(x_n - x_{D,n},\, y_n - y_{D,n}\right) \tag{18}$$

It is important to make sure that the outer normal direction is found, so we add π to the α value found from Eq. (18) if the profile is concave at the point of computation.

Next, we derive the formulation to determine the cam rotation angle and the corresponding follower displacement/angle for the most general forms of the common cam-follower mechanisms with the following five types of followers: (1) translating roller follower, (2) oscillating roller follower, (3) translating flat-faced follower, (4) oscillating flat-faced follower, and (5) translating/oscillating knife-edge follower.

3.1 Translating Roller Follower Case

The roller radius r_f and eccentricity e are known. We locate the fixed coordinate system in such a way that the Y axis points towards the follower and is parallel to the prismatic joint axis, as shown in Fig. 3. Notice that, since the data point measuring axes (O,x,y) is arbitrarily oriented, $\theta = 0°$ does not necessarily correspond to the lowest position of the follower.

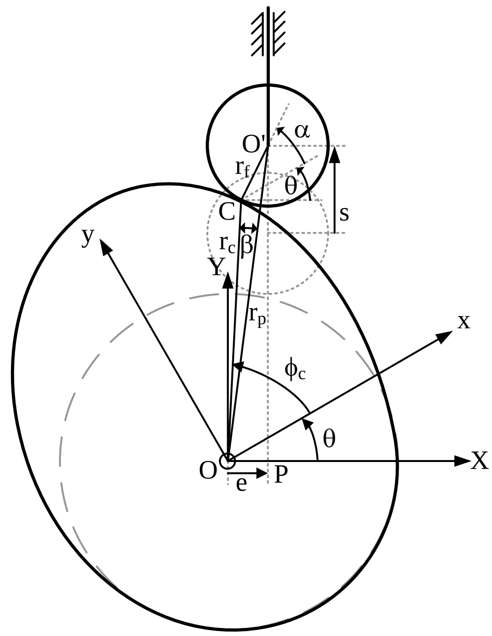

Fig. 3. Translating roller follower case

From the cosine and sine laws for triangle OCO', we have

$$r_p = \sqrt{r_c^2 + r_f^2 + 2r_c r_f \cos(\phi_c - \alpha)} \tag{19}$$

$$\beta = \sin^{-1}\frac{r_f \sin(\phi_c - \alpha)}{r_p} \tag{20}$$

Then from triangle OPO', we have

$$\theta = \cos^{-1}\frac{e}{r_p} - \phi_c + \beta \tag{21}$$

$$s = \sqrt{r_p^2 - e^2} - \sqrt{(r_b + r_f)^2 - e^2} \tag{22}$$

Eqs. (19) and (22) turn out to be the same as Eqs. (3) and (6), but the expressions for angles are different.

3.2 Oscillating Roller Follower Case

The roller radius r_f, the follower link length r_r, and the distance r_a between the revolute joints are known. We locate the fixed coordinate system in such a way that the Y axis points from the cam rotation center O to the follower rotation center Q, as shown in Fig. 4.

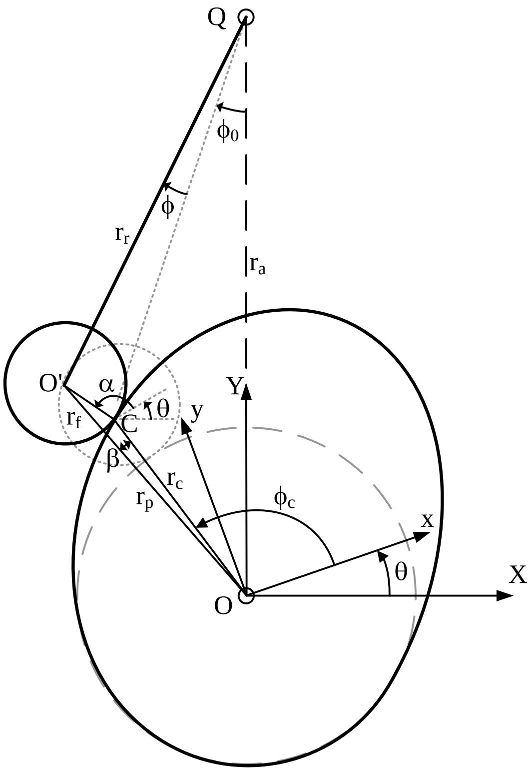

Fig. 4. Oscillating roller follower case

Eqs. (19) and (20) are also valid for this case. From the triangle OQO', the cam and follower rotation angles are found as

$$\theta = \cos^{-1}\frac{r_a{}^2 + r_p{}^2 - r_r{}^2}{2r_a r_p} + \frac{\pi}{2} - \phi_c + \beta \tag{23}$$

$$\phi = \cos^{-1}\frac{r_a{}^2 + r_r{}^2 - r_p{}^2}{2r_a r_r} - \cos^{-1}\frac{r_a{}^2 + r_r{}^2 - \left(r_b + r_f\right)^2}{2r_a r_r} \tag{24}$$

Compared to [10], Eqs. (8) and (24) are the same, but Eqs. (7) and (23) are different.

3.3 Translating Flat-Faced Follower Case

The acute flat-face angle γ is known. We locate the fixed coordinate system in such a way that the Y axis points towards the follower and is parallel to the prismatic joint axis, as shown in Fig. 5.

The cam rotation angle is straightforward in this case:

$$\theta = \gamma - \alpha \tag{25}$$

The follower displacement s is found by drawing a perpendicular OM from cam center O to the follower:

$$s = \left[r_c \cos\left(\phi_c - \alpha\right) - r_b\right]\sin\gamma \tag{26}$$

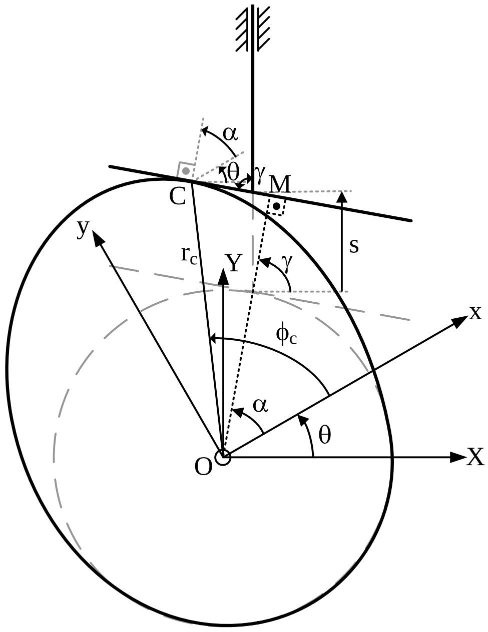

Fig. 5 Translating flat-faced follower

3.4 Oscillating Flat-Faced Follower Case

The eccentricity e on the follower and the distance r_a between the revolute joints are known. We locate the fixed coordinate system in such a way that the Y axis points from the cam rotation center O to the follower rotation center Q, as shown in Fig. 6.

We complete the follower part QPC to a rectangle ABCP such that the AB side is coincident with cam center O. Notice that $\measuredangle$ QOA = π – α – θ and that from triangle AOQ, |AQ| = r_a sin(α + θ). Because $\measuredangle$ BOC = $\phi_c - \alpha + \pi/2$, from the triangle BOC, we have

$$\theta = \pi - \sin^{-1}\frac{r_c\cos\left(\phi_c - \alpha\right) - e}{r_a} - \alpha \tag{27}$$

When the follower is tangent to the base circle,

$$\phi_0 = \sin^{-1}\frac{r_b - e}{r_a}$$

Summing up the angles around point P gives

$$\alpha + \theta + \pi/2 + \phi + \phi_0 = 3\,\pi/2$$

Therefore,

$$\phi = \pi - \alpha - \theta - \sin^{-1}\frac{r_b - e}{r_a} \tag{28}$$

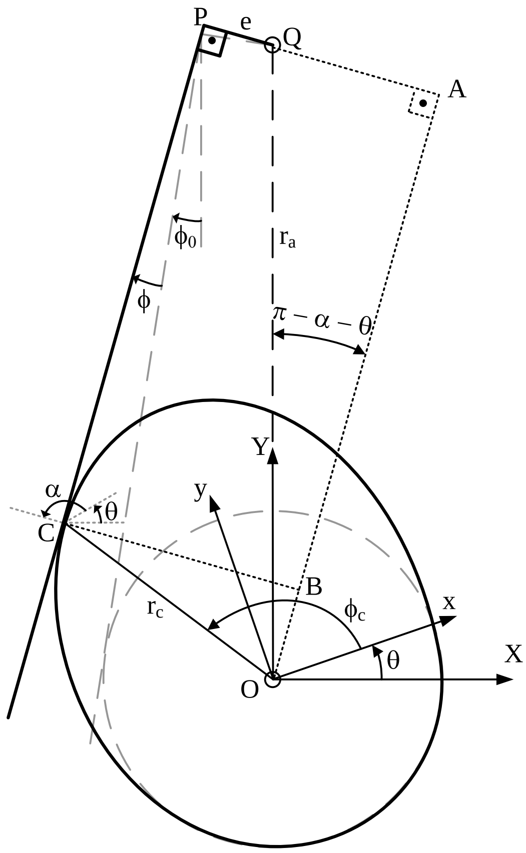

Fig. 6 Oscillating flat-faced follower case

3.5 Translating/Oscillating Knife-Edge Follower Case

The knife-edge follower can be considered as the limiting case of the roller follower. For the translating knife-edge follower case, as roller radius r_f approaches 0, $r_p = r_c$ and $\beta = 0°$ from Eqs. (19) and (20). Therefore, from Eqs. (21) and (22), we have

$$\theta = \cos^{-1}\frac{e}{r_c} - \phi_c \tag{29}$$

$$s = \sqrt{r_c^{\,2} - e^2} - \sqrt{r_b^{\,2} - e^2} \tag{30}$$

Similarly, for the oscillating knife-edge follower case, as roller radius r_f approaches 0, $r_p = r_c$ and $\beta = 0°$ from Eqs. (19) and (20). Therefore, from Eqs. (23) and (24), we have

$$\theta = \cos^{-1}\frac{r_a^{\,2} + r_c^{\,2} - r_r^{\,2}}{2 r_a r_c} + \frac{\pi}{2} - \phi_c \tag{31}$$

$$\phi = \cos^{-1}\frac{r_a^{\,2} + r_r^{\,2} - r_c^{\,2}}{2 r_a r_r} - \cos^{-1}\frac{r_a^{\,2} + r_r^{\,2} - r_b^{\,2}}{2 r_a r_r} \tag{32}$$

4. Computational Examples Using Excel

The formulas provided in Sections 2 & 3 are to be applied for $0 \le n \le N - 1$ for N data points on a cam profile. We implement the formulation in Excel for the analysis of cam profiles. The cam profiles used here are constructed analytically for the purpose of computing numerical errors. Regarding the use of Excel in mechanism analysis and synthesis, please refer to [12] for further information.

A snapshot of the Excel analysis sheet is illustrated in Fig. 7. Given (or having calculated) the cam profile coordinates in any desired increments of cam angle, the analyses are performed for four cases: translating/oscillating roller/flat-faced followers. The numerical errors between the exact output displacement diagrams and the computed ones are also tabulated.

Notice that, from the percentile error graph in Fig. 7, the numerical error peaks whenever the acceleration of the follower is discontinuous.

The following displacement diagrams are used in our analysis: the simple/double harmonic, parabolic, cycloidal, cubic (two types), trapezoidal, 3-4-5 & 4-5-6-7 polynomial, and dwell motions (see, for example, [13]). Among these motions, the cubic type 1 motion curve has the most extreme jump in acceleration and, as expected, the largest error is encountered when this curve is used. Hence we use this curve as a reference in our maximum error calculations.

Here is the example curve we used for our computations:

Rise H with cubic type 1 curve for $0° < \theta < 90°$
Fall H with cubic type 2 curve for $90° < \theta < 180°$
Rise H with parabolic curve for $180° < \theta < 270°$
Fall H with simple harmonic motion curve for
$270° < \theta < 360°$

Note that we use this curve because there are many large jumps in acceleration, as shown in Fig. 8.

The curves of cubic type 1, cubic type 2, parabolic, and simple harmonic motion (SHM) for the rise length H and the cam angle range $0 < \theta < \beta$ are given in Table 1.

The values H = 40 units and H = 20° are used for translating and oscillating followers, respectively. A typical follower displacement, velocity, and acceleration variation together with the percentile error between the exact output displacement and the computed one are depicted in Fig. 9. The velocity and acceleration are computed using finite differences, and the profile is obtained by the cubic type 1, cubic type 2, parabolic, and SHM displacement curves.

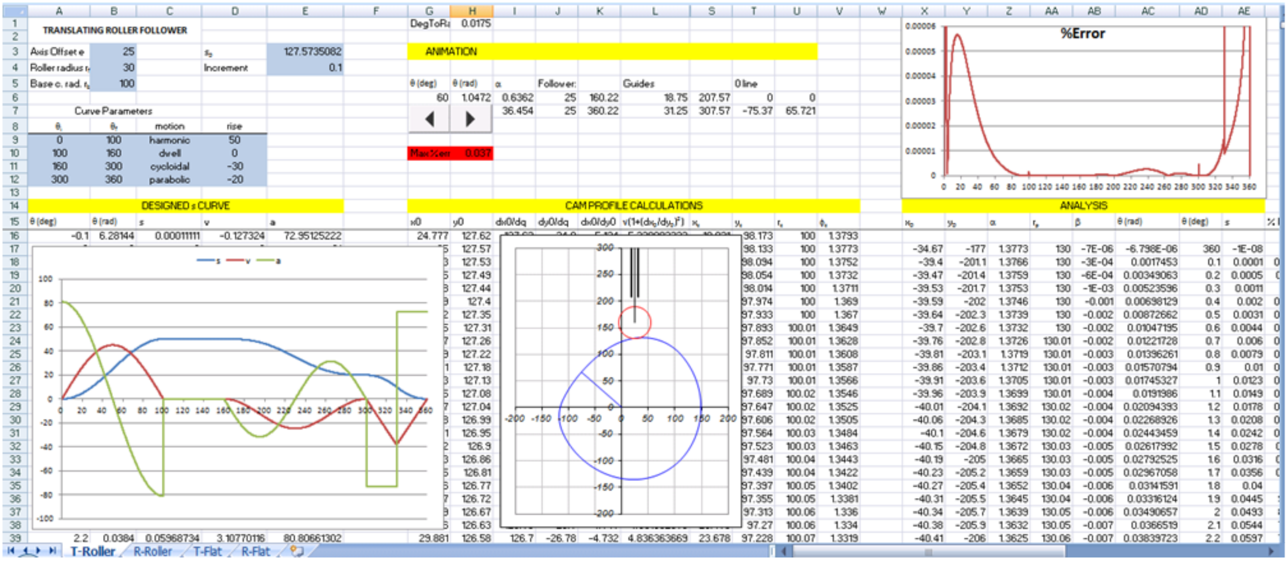

Fig. 7 A snapshot of the Excel sheet

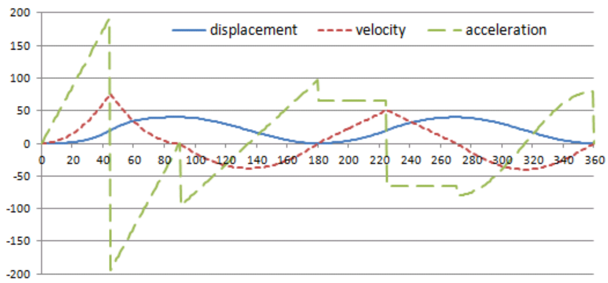

Fig. 8 Example motion diagram

Table 1 Displacement curve definitions [13]

Motion	Curve
Cubic1	$s=\begin{cases} 4H(\theta/\beta)^3 & \text{for } 0<\theta<\beta/2 \\ H\left[1-4(1-\theta/\beta)^3\right] & \text{for } \beta/2<\theta<\beta \end{cases}$
Cubic2	$s=H(\theta/\beta)^2(3-2\theta/\beta)$
Parabolic	$s=\begin{cases} 2H(\theta/\beta)^2 & \text{for } 0<\theta<\beta/2 \\ H\left[1-2(1-\theta/\beta)^2\right] & \text{for } \beta/2<\theta<\beta \end{cases}$
SHM	$s=(H/2)\left[1-\cos(\pi\theta/\beta)\right]$

It can be seen that, in Fig. 9 (a), the acceleration jumps occur at 0°, 45°, 90°, 180°, 225° and 270°. Due to discontinuities in acceleration, we have peaks in errors around 0°, 45°, 180° and 225° cam angles. These errors cannot be easily observed from the computed displacement variation.

We analyze the cases where the cam profile coordinates are given in every 5°, 2°, 1°, 0.5°, and 0.1° cam angles. In what follows, we summarize some results regarding errors for different follower types.

(a)

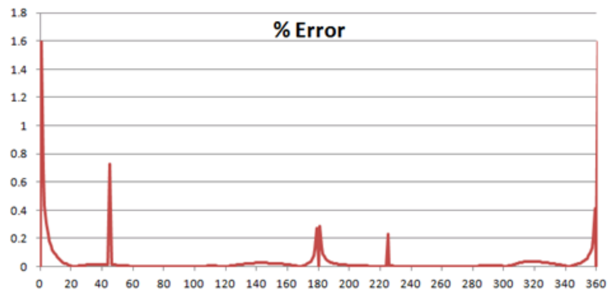

(b)

Fig. 9 (a) The computed motion profile and (b) the percentile error of displacement for the oscillating roller follower case with 360 data points

Translating Roller Follower

This case is analyzed for base radius r_b = 120, roller radius r_f = 30, and eccentricity e = 50. The errors obtained for different cam angle increments are listed in Table 2.

Table 2 Errors for the translating roller follower case

Increment	5°	2°	1°	0.5°	0.1°
Max. % Error	4.07	0.78	0.88	0.44	0.09
Occurs at cam angle	45°	2°	45°	45°	45°

As shown in Table 2, smaller increments do not necessarily imply smaller maximum errors. In this case the maximum error mostly occurs around cam angle 45°, where the largest jump in acceleration occurs.

Oscillating Roller Follower

This case is analyzed for the following dimensions: base radius r_b = 150, roller radius r_f = 30, arm length r_r = 200, and fixed length r_a = 250. The errors obtained for different cam angle increments are listed in Table 3.

Table 3 Errors for oscillating roller follower case

Increments	5°	2°	1°	0.5°	0.1°
Max. % Error	2.28	0.94	0.48	0.24	0.05
Occurs at cam angle	5°	2°	1°	0.5°	0.1°

In this case the maximum error always occurs at the beginning of the cycle. This error is likely due to the low numerical precision of Excel when dealing with the small follower displacement angle. This error can be decreased by using other computation tools other than Excel and employing higher number precisions.

Translating Flat-Faced Follower

This case is analyzed for base radius r_b = 180 and face angle γ = 80°. The errors obtained for different cam angle increments are listed in Table 4.

Table 4 Errors for translating flat-faced follower case

Increment	5°	2°	1°	0.5°	0.1°
Max. % Error	18.4	5.62	3.75	1.81	0.34
Occurs at cam angle	45°	46°	45°	45°	45

Again, the maximum error appears around cam angle 45°, where the largest jump in acceleration occurs.

Oscillating Flat-Faced Follower

This case is analyzed for base radius r_b = 200, fixed length r_a = 250, and eccentricity e = 0. The errors obtained for different cam angle increments are listed in Table 5.

Table 5 Errors for oscillating flat-faced follower case

Increment	5°	2°	1°	0.5°	0.1°
Max. % Error	6.52	3.06	1.59	0.81	0.16
Occurs at cam angle	5°	2°	1°	0.5°	0.1°

For the other three cases, the formulas in Sections 2 and 3 (with or without kinematic inversion) result in comparable error values. However, for this case, the formulation with kinematic inversion yields much smaller error values. The error values in Table 5 are from the analysis without kinematic inversion.

5. Conlusion

This paper investigates the kinematic analysis of planar cam follower mechanisms when the cam profiles and follower types are given. We utilized a systematic approach based on the existence of a common normal at the contact point between a cam and its follower. We studied six follower types: translating/rotating roller/flat-faced/knife-edge followers. Error analyses regarding different increments of discrete data points were conducted, and, as predicted, error peaked where the acceleration of the follower is discontinuous. Of course, in practice, there are several other error sources, such as manufacturing errors, wear of the pieces, and measurement errors. However, as far as the errors due to the analysis algorithm proposed in this paper and computational errors are considered, we can conclude that the displacement diagram can be successfully predicted when the original diagram is constructed with one of the known motion profiles.

We believe the formulation discussed in this paper serves as a convenient tool for practicing engineers and as a straightforward aide for students studying planar cam follower mechanisms.

Acknowledgements

The authors would like to express their gratitude to the Engineering School of National Cheng Kung University for the financial support of Dr. Gokhan Kiper's visiting research program in Taiwan. The assistance from Mr. Chih-Hsun Wu of National Cheng Kung University in testing the algorithm is also acknowledged.

References

[1] Andrews Products Inc., EZCAM Inspection Equipment Catalog, 2002, available online at http://www.andrewsproducts.com/Downloads/andrews_ezcam.pdf.

[2] TecQuipment Ltd., TM21 – Cam Analysis Machine, 2008, available online at http://www.tecquipment.com/Datasheets/TM21_0908.pdf.

[3] Performance Trends Inc., Electronic Camshaft (cam) Test Measurement Stand with Program Software, http://performancetrends.com/cam_test_stand.htm, accessed: 24.05.2012.

[4] Performance Trends Inc., Cam Analyzer – Camshaft Measuring Analysis Software Program, http://performancetrends.com/ca20.htm, accessed 24.05.2012.

[5] W. Wunderlich, Contributions to the Geometry of Cam Mechanisms with Oscillating Followers, Journal of Mechanisms, Vol. 6, No. 1, pp. 1-20, 1971.

[6] J. Angeles and C. S. López-Cajún, Optimization of Cam Mechanisms, Kluwer Academic Publishers, Dordrecht / Boston / London, 1991.

[7] C. F. Reinholtz, S. G. Dhande and G. N. Sandor, Kinematic Analysis of Planar Higher Pair Mechanisms, Mechanism and Machine Theory, Vol. 13, No. 6, pp. 619-629, 1978.

[8] R. H. Fries and C. A. Rogers, Predictions of Cam Wear Profiles, in: D. Dowson, C. M. Taylor, M. Godet, D

Berthe (Eds.), Tribological Design of Machine Elements, Elsevier Science Publishers B. V., pp. 101-109, 1989.
[9] P. Kirwan, Construction of Cam and Follower Systems, http://www3.ul.ie/~kirwanp/condd.htm, accessed 05.06.2012.
[10] B. Tutak and E. Söylemez, Kam Profili Koordinatlarından Uydu Hareketinin Bulunması, Proc. TÜBİTAK 2. Ulusal Makina Teorisi Sempozyumu, Gaziantep (Turkey), pp. 27-35, 1986.
[11] Wikipedia: The Free Encyclopedia, Circumscribed Circle, http://en.wikipedia.org/wiki/Circumscribed_circle, accessed 28.05.2012.
[12] E. Söylemez, Using Computer Spreadsheets in Teaching Mechanisms, in: M. Ceccarelli (Ed.), Proceedings of EUCOMES 08 – The Second European Conference on Mechanism Science, Springer, pp. 45-53, 2009.
[13] E. Söylemez, Basic Cam Motion Curves, in: Mechanisms – Middle East Technical University Open Courseware, available online at, http://ocw.metu.edu.tr/pluginfile.php/6886/mod_resource/content/1/ch8/8-3.htm, accessed: 06.06.2012.